Charge Transfer and Delocalization in Conjugated (Ferrocenylethynyl)oligothiophene Complexes

Yongbao Zhu and Michael O. Wolf*

Contribution from the Department of Chemistry, The University of British Columbia, Vancouver, British Columbia, Canada V6T 1Z1

Received March 9, 2000. Revised Manuscript Received August 4, 2000

Abstract: A series of conjugated mono(ferrocenylethynyl)oligothiophene and bis(ferrocenylethynyl)oligothiophene complexes have been prepared. The cyclic voltammograms of the complexes all contain a reversible ferrocene oxidation wave and an irreversible oligothiophene-based wave. The potential difference between the two waves (ΔE) varies from 0.38 to 1.12 V, depending on the length and substitution of the oligothiophene group. Several of the mono(ferrocenylethynyl)oligothiophene complexes couple when oxidized, resulting in the deposition of a redox-active film on the electrode surface. In solution, electrochemical oxidation of the Fe^{II} centers yields the corresponding monocations and dications, which exhibit oligothiophene-to-Fe^{III} charge-transfer transitions in the near-IR region. The band maxima of these low-energy transitions correlate linearly with ΔE, while the oscillator strengths show a linear correlation with negative slope with ΔE. The complexes with similar charge-transfer transition dipole lengths show an increase in the extent of charge delocalization with smaller ΔE. Comparisons between complexes with different length oligothiophene ligands show that a reduction in ΔE results either in greater delocalization of charge or in charge being delocalized further along the rigid oligothiophene ligand. These results have important implications in understanding charge delocalization in metal-containing polymers.

Introduction

Polythiophene is a conjugated polymer with many interesting optical and electronic properties such as electrochromism and near-metallic conductivity.[1] Oligomers of thiophene are also technologically important materials, for example, hexathiophene has an extraordinarily high charge mobility and has been used in prototype organic thin-film transistors.[2] Interest in materials with these properties has directed substantial efforts toward the preparation of substituted oligo- and polythiophenes, and some studies have focused on materials in which metal groups are pendant to or inserted in the backbone.[3−16] Metal groups often possess redox and optical properties which can significantly influence the electronic behavior of an oligo- or polythiophene backbone to which they are coupled.

Electronic conductivity in conjugated organic polymers such as polythiophene depends on delocalization of charge along the polymer backbone.[1] In polymers containing both metal centers and conjugated bridges, delocalization along the backbone is expected to enhance conductivities and charge mobilities relative to analogous polymers in which charge is localized. In such materials, the extent of charge delocalization will depend on the magnitude of the energy barriers to charge transfer along the backbone. One approach to achieve more extensive delocalization is to use conjugated bridges and metal centers with similar oxidation potentials; in this way the energy barrier for charge transfer between the metal and bridging groups should be reduced.[15−19]

In previous studies, we have demonstrated that in oligomers and polymers in which the gap between metal and organic bridge oxidation potentials is small, a low-energy ligand-to-metal charge transfer (LMCT) band appears in the near-IR region upon oxidation.[10,11] Similar bands are frequently observed in mixed-valent complexes, and have been analyzed to assess the extent of charge delocalization in these complexes.[20,21] Insight into the delocalization in metal-containing conjugated polymers may be obtained using a similar analysis of the LMCT bands in these

(1) Skotheim, T. A.; Elsenbaumer, R. L.; Reynolds, J. R. *Handbook of Conducting Polymers,* 2nd ed.; Marcel Dekker: New York, 1998.
(2) Torsi, L.; Dodabalapur, A.; Rothberg, L. J.; Fung, A. W. P.; Katz, H. E. *Science* **1996**, *272*, 1462−1464.
(3) Zotti, G.; Zecchin, S.; Schiavon, G.; Berlin, A.; Pagani, G.; Canavesi, A. *Chem. Mater.* **1995**, *7*, 2309−2315.
(4) Wolf, M. O.; Wrighton, M. S. *Chem. Mater.* **1994**, *6*, 1526−1533.
(5) Segawa, H.; Wu, F. P.; Nakayama, N.; Maruyama, H.; Sagisaka, S.; Higuchi, N.; Fujitsuka, M.; Shimidzu, T. *Synth. Met.* **1995**, *71*, 2151−2154.
(6) Reddinger, J. L.; Reynolds, J. R. *Macromolecules* **1997**, *30*, 673−675.
(7) Zhu, S. S.; Kingsborough, R. P.; Swager, T. M. *J. Mater. Chem.* **1999**, *9*, 2123-2131.
(8) Kingsborough, R. P.; Swager, T. M. *Adv. Mater.* **1998**, *10*, 1100−1104.
(9) Kingsborough, R. P.; Swager, T. M. *Prog. Inorg. Chem.* **1999**, *48*, 123−231.
(10) Zhu, Y. B.; Wolf, M. O. *Chem. Mater.* **1999**, *11*, 2995−3001.
(11) Zhu, Y. B.; Millet, D. B.; Wolf, M. O.; Rettig, S. J. *Organometallics* **1999**, *18*, 1930−1938.
(12) Higgins, S. J.; Jones, C. L.; Francis, S. M. *Synth. Met.* **1999**, *98*, 211−214.
(13) Vidal, P.-L.; Divisia-Blohorn, B.; Bidan, G.; Kern, J.-M.; Sauvage, J.-P.; Hazemann, J.-L. *Inorg. Chem.* **1999**, *38*, 4203−4210.
(14) Ley, K. D.; Schanze, K. S. *Coord. Chem. Rev.* **1998**, *171*, 287−307.
(15) Zhu, S. S.; Carroll, P. J.; Swager, T. M. *J. Am. Chem. Soc.* **1996**, *118*, 8713−8714.
(16) Zhu, S. S.; Swager, T. M. *J. Am. Chem. Soc.* **1997**, *119*, 12568−12577.
(17) Desjardins, P.; Yap, G. P. A.; Crutchley, R. J. *Inorg. Chem.* **1999**, *38*, 5901−5905.
(18) Evans, C. E. B.; Ducharme, D.; Naklicki, M. L.; Crutchley, R. J. *Inorg. Chem.* **1995**, *34*, 1350−1354.
(19) Evans, C. E. B.; Naklicki, M. L.; Rezvani, A. R.; White, C. A.; Kondratiev, V. V.; Crutchley, R. J. *J. Am. Chem. Soc.* **1998**, *120*, 13096−13103.
(20) Hush, N. S. *Prog. Inorg. Chem.* **1967**, *8*, 391−444.
(21) Crutchley, R. J. *Adv. Inorg. Chem.* **1994**, *41*, 273−325.

10.1021/ja0008564 CCC: $19.00
Published on Web 09/29/2000

materials. We report herein the spectroscopic and electrochemical characterization of a series of compounds in which a metal redox group (ferrocene) is conjugated to oligothiophenes of varying oxidation potentials (**1a**−**e** and **2a**−**e**). Analysis of these data allows conclusions to be made regarding charge delocalization in these complexes.

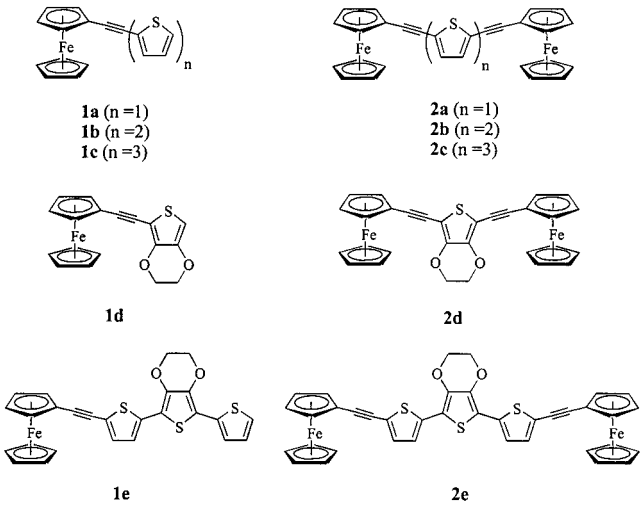

Experimental Section

Syntheses. Compounds **1a**−**e** and **2a**−**e** were all prepared by coupling ethynylferrocene with the appropriate mono- or dibromooligothiophene using $Pd(PPh_3)_2Cl_2$ and CuI catalysts. The preparation of **2a**−**c** has also been recently reported by Lin and co-workers.[22] The compounds were purified either by chromatography on silica gel or by recrystallization from CH_2Cl_2/hexanes or toluene, and were characterized using ^1H and ^{13}C NMR, UV−vis and mass spectroscopies, as well as C, H elemental analyses. For complete details see the Supporting Information.

Electrochemistry. Electrochemical measurements were conducted on a Pine AFCBP1 bipotentiostat using a Pt disk electrode with a diameter of 1.0 mm, a Pt coil wire counter electrode, and a Ag wire reference electrode. The supporting electrolyte, $[(n\text{-}Bu)_4N]PF_6$, was purified by recrystallization three times from hot ethanol and dried in vacuo at 100 °C for 1 week. Methylene chloride was dried by heating at reflux over calcium hydride, followed by distillation. Decamethylferrocene (−0.12 V vs SCE) was used as an internal standard for the electrochemical experiments. Cyclic voltammograms were obtained under nitrogen at room temperature in a methylene chloride solution containing $4-6 \times 10^{-3}$ M complex and 0.5 M $[(n\text{-}Bu)_4N]PF_6$. Before addition of dry solvent the cells containing the electrodes and electrolyte were dried in vacuo at 90 °C overnight. Electrolyses of **1a**−**e** and **2a**−**e** were conducted in a CH_2Cl_2 solution containing 0.10 M $[(n\text{-}Bu)_4N]PF_6$ using Pt mesh electrodes and a $Ag/AgNO_3$ (CH_3CN) reference electrode (0.39 V vs SCE). UV−vis−near-IR spectra of solutions of $\mathbf{1a}^+$−$\mathbf{e}^+$ and $\mathbf{2a}^{2+}$−$\mathbf{e}^{2+}$ in CH_2Cl_2 containing 0.10 M $[(n\text{-}Bu)_4N]PF_6$ were obtained on a Varian Cary 5 spectrometer.

Results

Cyclic Voltammetry. Complexes **1a**−**e** and **2a**−**e** all contain ferrocenyl and oligothiophene groups which are both expected to show redox activity. The reversibility and relative oxidation potentials of the redox processes in these compounds were determined by cyclic voltammetry in CH_2Cl_2 solution containing 0.5 M $[(n\text{-}Bu)_4N]PF_6$. All the compounds have two oxidation waves in the range 0−1.8 V vs SCE (shown for **1a**−**e** in Figure 1), and the potentials for these waves are collected in Table 1. The first oxidation wave is reversible and occurs at a potential very close to that of the $Fe^{II/III}$ couple in ethynylferrocene ($E_{1/2}$ = 0.57 V vs SCE), therefore this wave is assigned to the $Fe^{II/III}$ redox couple.

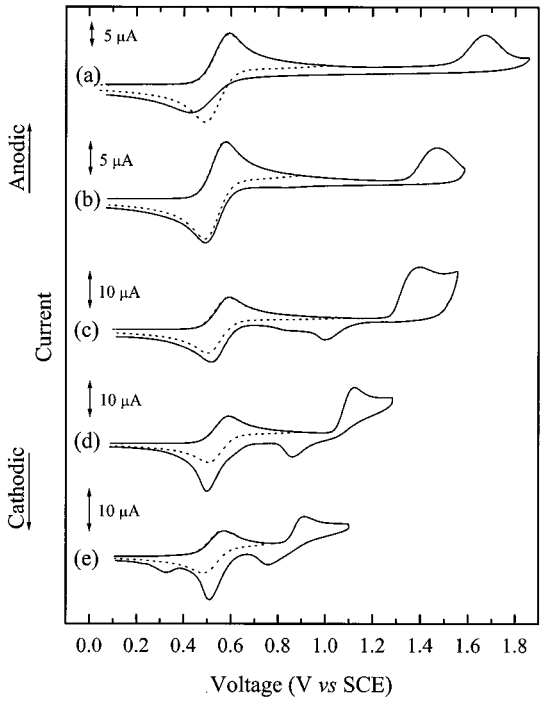

Figure 1. Cyclic voltammetry of (a) **1a**, (b) **1d**, (c) **1b**, (d) **1c**, and (e) **1e** in CH_2Cl_2 containing 0.5 M $[(n\text{-}Bu)_4N]PF_6$. Scan rate = 100 mV/s.

Table 1. Electrochemical and UV−Vis Absorption Data

complex	$^1E_{1/2}$ ± 0.01 (V)[a]	$^2E_{p,a}$ ± 0.01 (V)[a]	ΔE ± 0.02 (V)[a,b]	λ_{max} (nm) (ϵ ($M^{-1}cm^{-1}$))[c]
1a	0.55	1.67	1.12	305 (14000), 445 (610)
1b	0.55	1.40	0.85	350 (25000), 445 (1600) (sh)
1c	0.55	1.13	0.58	392 (35000)
1d	0.53	1.47	0.94	310 (13000), 445 (610)
1e	0.53	0.91	0.38	406 (39000)
2a	0.56	1.68	1.12	342 (26000), 446 (3300) (sh)
2b	0.55	1.42	0.87	390 (38000)
2c	0.55	1.23	0.68	416 (44000)
2d	0.56	1.50	0.94	352 (27000), 448 (3700) (sh)
2e	0.54	1.04	0.50	433 (52000)

[a] Volts vs SCE, Pt working electrode, CH_2Cl_2 containing 0.5 M $[(n\text{-}Bu)_4N]PF_6$, 20 °C. [b] $\Delta E = [^2E_{p,a} - {}^1E_{1/2}]$. [c] CH_2Cl_2 solution. sh = shoulder.

The voltammograms of the compounds containing two ferrocenyl groups (**2a**−**e**) show only a single oxidation wave for these centers, indicating that there is little direct interaction between the metal centers over the conjugated oligothiophene bridge. Interactions between metal centers have been observed for other complexes in which conjugated bridges link two ferrocenyl groups, and are sensitive to the nature and length of the bridge.[23] In the series of all-trans compounds $Fc(CH{=}CH)_nFc$ (n = 1−6, Fc = ferrocenyl),[24] peak separations are observed only for $n \leq 3$, while for $FcCH{=}CHC_6H_4CH{=}CHFc$ no peak separation is observed.[25] Thus, it is not surprising that

(22) Thomas, K. R. J.; Lin, J. T.; Wen, Y. S. *Organometallics* **2000**, *19*, 1008−1012.

(23) Barlow, S.; O'Hare, D. *Chem. Rev.* **1997**, *97*, 637−669.

(24) Ribou, A.-C.; Launey, J.-P.; Sachtleben, M. L.; Li, H.; Spangler, C. W. *Inorg. Chem.* **1996**, *35*, 3735−3740.

(25) Morrison, W. H.; Krogsrnd, S.; Hendrickson, D. N. *Inorg. Chem.* **1973**, *12*, 1998−2004.

peak separations are not observed in **2a**−**e**, in which the Fe−Fe distances are considerably longer.

Several studies have shown substantial electronic interactions may still occur in cases where a conjugated organic bridge links metal centers, even in the absence of any observable peak separation. Pickup has examined electronic communication in hybrid metallopolymers bearing bis(2,2′-bipyridyl)Ru moieties on a conjugated backbone.[26,27] Despite small $Ru^{II/III}$ peak separations in the voltammetry of these materials, electron diffusion coefficients are greater than those for comparable nonconjugated materials by an order of magnitude. In several of the transition-metal containing conjugated polymers prepared by Swager, redox-matching between the metal and organic components resulted in enhanced conductivities despite the absence of peak separation in the metal redox waves.[8,15,16]

The second oxidation wave in the voltammograms of all the compounds is irreversible (Figure 1), and the oxidation potential depends strongly on the nature of the oligothiophene group. Both longer conjugation length and the presence of electron-donating ethylenedioxy substituents (in **1d**, **1e**, **2d**, and **2e**) results in a decrease in the potential of this wave. On the basis of these observations the second wave is assigned to an oligothiophene-based oxidation, the potential of which varies from 0.91 to 1.68 V vs SCE. The peak current of the second wave varies due to differences in the stabilities of the resulting cations.

The cyclic voltammograms of **1b**, **1c**, and **1e** (Figure 1c−e) all contain new reduction waves which appear after the first scan past the irreversible thiophene oxidation wave. In subsequent scans, these reduction waves have corresponding oxidation features, and when solutions of these compounds are cycled repeatedly past the thiophene oxidation wave (0.7−1.5 V vs SCE for **1b**, 0−1.3 V for **1c**, and 0−1.1 V for **1e**), an electrochromic film deposits on the electrode surface. Both anodic and cathodic currents increase with scan number, clearly indicating that the deposited films are conductive. The films are orange-red in the neutral state, and are black when fully oxidized. Characterization of the deposited poly-**1b**, poly-**1c**, and poly-**1e** films by cyclic voltammetry in monomer-free solution reveals a reversible wave at ∼0.5 V vs SCE due to the $Fe^{II/III}$ couple as well as other waves assigned to thiophene-based oxidations (Figure 2).

Thiophene derivatives containing unsubstituted α positions typically undergo oxidative coupling at this position.[28] Blocking this position with substituents such as alkyl groups prevents oxidative coupling, and thiophene derivatives with one blocked and one unblocked α position, such as α-methyloligothiophenes, undergo coupling to produce dimers.[29] The similarity of the electrochemical behavior of the α-methyloligothiophenes to that of **1a**−**e** suggests that the electrodeposited films consist primarily of α,α-coupled dimers. The oxidation wave at 1.01 V in the voltammogram of poly-**1b** (Figure 2a) occurs at a lower potential than the oxidation of the terthiophene group in **2c**. This is consistent with the presence of a longer tetrathiophene bridge in poly-**1b**. The small reduction wave at 0.63 V vs SCE may be due to the presence of longer oligomers or polymers resulting from some additional α,*β* or *β*,*β* coupling. Due to the insolubility of the films, further characterization by either NMR or MS methods was unsuccessful. Although the second oxidation waves of **1a** and **1d** are completely irreversible, no new reduction waves which would be evidence of coupling are observed in these cases.

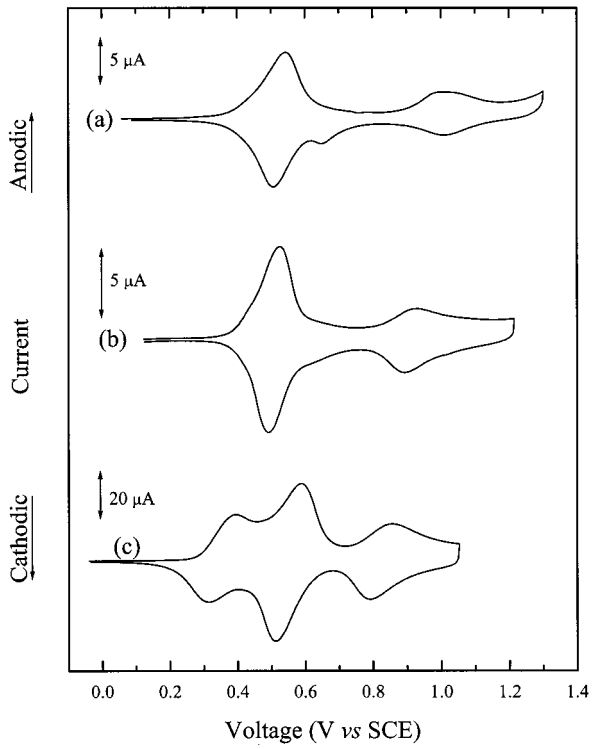

Figure 2. Cyclic voltammetry of (a) poly-**1b**, (b) poly-**1c**, and (c) poly-**1e** in CH_2Cl_2 containing 0.5 M $[(n\text{-}Bu)_4N]PF_6$. Scan rate = 100 mV/s.

The cyclic voltammograms of deposited poly-**1c** and poly-**1e** films (Figure 2b and 2c) contain two and three oxidation waves, respectively. The potentials at which these waves appear suggests that these materials are also primarily α,α coupled dimers, although other coupling pathways to yield longer oligomers or polymers cannot be excluded. In these films, α,α coupling would result in a hexathiophene bridge linking the ferrocenyl groups. Thiophene oligomers of this length are able to support two reversible one-electron oxidations, for instance, in didodecylhexathiophene the first oxidation occurs at 0.65 V vs SCE with a second wave at 0.85 V vs SCE.[30] The waves at 0.35 and 0.82 V vs SCE in the cyclic voltammogram of poly-**1e** are therefore assigned as sequential, reversible oxidations of the substituted hexathiophene bridge. In poly-**1c** the first thiophene oxidation wave overlaps the ferrocenyl wave at 0.51 V. The electron-donating ethylenedioxy groups in poly-**1e** result in lower potential waves for the bridge compared to poly-**1c**, in fact the first thiophene oxidation in this material occurs at a lower potential than for the ferrocenyl groups, and it is possible that an increase in the conductivity due to p-doping of the molecular wire linking the two metal groups could lead to enhanced interaction between these groups; however, peak splitting is not observed in this case.

For complexes **2a**, **2b**, and **2d** the oligothiophene oxidation waves are irreversible, and no new reduction waves are observed; however, for **2c** and **2e** the second oxidation waves are more reversible at higher scan rates, and new reduction features appear (see Supporting Information). For example, at a scan rate of 100 mV/s a small reduction wave was observed at 0.96 V for **2c** and at 0.64 V vs SCE for **2e**. This wave is likely due to the reduction of a product resulting from coupling of **2c** or **2e** upon scanning past the oligothiophene oxidation potential, analogous to the behavior of **1c**, **1d**, and **1e**. Although the disubstituted complexes do not have unsubstituted α

(26) Cameron, C. G.; Pickup, P. G. *Chem. Commun.* **1997**, 303−304.
(27) Cameron, C. G.; Pickup, P. G. *J. Am. Chem. Soc.* **1999**, *121*, 11773−11779.
(28) Roncali, J. *Chem. Rev.* **1992**, *92*, 711−738.
(29) Zotti, G.; Schiavon, G.; Berlin, A.; Pagani, G. *Chem. Mater.* **1993**, *5*, 430−436.
(30) Bäuerle, P.; Segelbacher, U.; Gaudl, K.-U.; Huttenlocher, D.; Mehring, M. *Angew. Chem., Int. Ed. Engl.* **1993**, *32*, 76−78.

Table 2. UV−Vis−Near-IR Data for Oxidized Complexes

complex	UV−vis−near-IR λ_{max} (nm) ($\pm$ 5 nm) (ϵ (M^{-1} cm^{-1}))[a]
1a$^+$	280 (18000), 370 (5000) (sh), 875 (630 $\pm$ 20)
1b$^+$	340 (22000), 445 (8800) (sh), 1015 (1390 $\pm$ 50)
1c$^+$	385 (26000), 485(11000) (sh), 1090 (1550 $\pm$ 70)
1d$^+$	285 (23000), 410 (56000) (sh), 995 (1190 $\pm$ 50)
1e$^+$	400 (28000), 505 (12000) (sh), 1290 (2090 $\pm$ 90)
2a^{2+}	285 (29000), 425 (12000) (sh), 885 (1550 $\pm$ 60)
2b^{2+}	375 (28000), 475 (19000), 1010 (2600 $\pm$ 100)
2c^{2+}	410 (33000), 475 (29000) (sh), 1080 (3600 $\pm$ 160)
2d^{2+}	290 (28000), 320 (24000) (sh), 450 (14000) (sh), 985 (2400 $\pm$ 90)
2e^{2+}	425 (30000), 520 (25000) (sh), 1255 (4000 $\pm$ 150)

[a] CH_2Cl_2 containing 0.10 M [(*n*-Bu)$_4$N]PF_6, 20 °C. sh = shoulder.

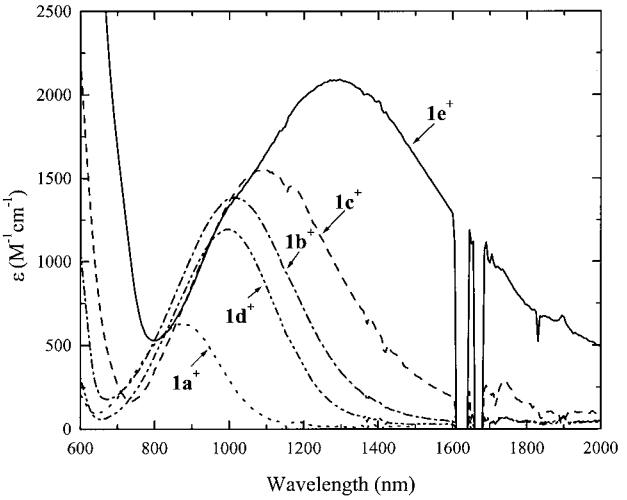

Figure 3. Vis−near-IR spectra of **1a**$^+$−**e**$^+$ in CH_2Cl_2 containing 0.1 M [(*n*-Bu)$_4$N]PF_6.

positions available, it is possible that these compounds form dimers or polymers by β,β coupling.

Electronic Spectroscopy. The UV−visible spectra of **1a**−**e** and **2a**−**e** all contain very strong absorption bands with λ_{max} between 305 and 433 nm assigned to an oligothiophene $\pi-\pi^*$ transition (Table 1). As expected, the absorption red-shifts and becomes more intense with an increase in the length of the oligothiophene group. The presence of the electron-donating ethylenedioxy groups results in a slight decrease in the absorption maximum relative to the unsubstituted compound with an equally long oligothiophene group. Several of the compounds also have a weaker absorption band at ~446 nm, assigned to an Fe^{II} d−d transition.[31] This band is not observed in the spectrum of the complexes containing longer oligothiophene groups because of overlap from the strong, broad $\pi-\pi^*$ transition of the oligothiophene group.

Stable solutions of the oxidized species **1a**$^+$−**e**$^+$ and **2a**$^{2+}$−**e**$^{2+}$ in CH_2Cl_2 containing 0.10 M [(*n*-Bu)$_4$N]PF_6 were prepared by constant potential electrolysis 0.25 V above $E_{1/2}$ of the ferrocenyl wave. For **1e** electrolysis was conducted 0.15 V above the ferrocenyl potential to preclude oxidation of the oligothiophene group. The UV−vis−near-IR spectra of these solutions were measured, and the data collected in Table 2. All the complexes have a strong absorption band with λ_{max} between 280 and 425 nm, with a low-energy shoulder between 370 and 520 nm. The high-energy absorption appears at a similar wavelength and is of comparable intensity to that observed in the corresponding neutral complexes, and these bands are therefore assigned as $\pi-\pi^*$ transitions in the oligothiophene groups. The shoulders observed between 370 and 520 nm are due to Cp → Fe^{III} ligand-to-metal charge-transfer (LMCT) transitions, and have been observed previously at similar energies in related compounds.[10,32]

The spectra of **1a**$^+$−**e**$^+$ and **2a**$^{2+}$−**e**$^{2+}$ also all contain broad, low-energy absorption bands with λ_{max} between 875 and 1290 nm (shown for **1a**$^+$−**e**$^+$ in Figure 3). These absorption bands are assigned to oligothiophene → Fe^{III} LMCT transitions. Similar low-energy transitions have also been observed in other Ru^{III} and Fe^{III} complexes with conjugated oligothiophene ligands.[10,11] The energy maxima of these LMCT transitions correlates to the length of the oligothiophene groups, with the absorption maxima shifting to lower energy with increased conjugation. The ethylenedioxy substituent in compounds with identical conjugation lengths (for example **1c** vs **1e**) results in a shift to lower energy and an increase in the intensity of the absorption band.

Discussion

We interpret the electrochemical and spectroscopic results reported herein using the classical electron-transfer model of Hush in which the electron is coupled between donor and acceptor via a single oscillator having the same frequency in both initial and final states.[20,21,33,34] Originally developed for interpretation of intervalence charge transfer (IVCT) in extended solids, the Hush model has been extended and applied to charge transfer in mixed-valent organometallic[35,36] and organic compounds,[37,38] as well as to LMCT and metal-to-ligand charge-transfer (MLCT) processes.[17,18,39]

The absorption maximum (ν_{max}) of a charge-transfer band has been related to the difference in electrochemical potentials (ΔE) between ligand (donor) and metal (acceptor) for the LMCT transition in Ru^{III} complexes (eq 1).[18,40] Here D corrects for the difference between the $Ru^{II/III}$ potential with an oxidized ligand attached and the measured $Ru^{II/III}$ oxidation potential, and χ is the sum of the inner and outer reorganizational parameters.

$$\nu_{max} = \Delta E + D + \chi \qquad (1)$$

A plot of ν_{max} vs ΔE will be linear if D and χ are constant for a series of complexes in which only the oxidation potential of the ligand varies. Such plots for **1a**$^+$−**e**$^+$ and **2a**$^{2+}$−**e**$^{2+}$ show linear correlations ($\nu_{max} = [4.4 \times 10^3](\Delta E) + 6.2 \times 10^3$ with $R = 0.98$ for **1a**$^+$−**e**$^+$ and $\nu_{max} = [5.1 \times 10^3](\Delta E) + 5.6 \times 10^3$ with $R = 0.99$ for **2a**$^{2+}$−**e**$^{2+}$, see Supporting Information). These correlations indicate that in these series a smaller difference in the donor and acceptor oxidation potentials results in a lower optical transition energy. Such correlations have been previously observed for other charge-transfer transitions.[18,40−42]

The extinction coefficient of the LMCT transition in the oxidized complexes clearly increases with smaller ΔE. Assum-

(31) Geoffroy, G. L.; Wrighton, M. S. *Organometallic Photochemistry*; Academic Press: New York, 1979.

(32) Sohn, Y. S.; Hendrickson, D. N.; Gray, H. B. *J. Am. Chem. Soc.* **1971**, *93*, 3603−3612.

(33) Creutz, C. *Prog. Inorg. Chem.* **1983**, *30*, 1−73.

(34) Barbara, P. F.; Meyer, T. J.; Ratner, M. A. *J. Phys. Chem.* **1996**, *100*, 13148−13168.

(35) Colbert, M. C. B.; Lewis, J.; Long, N. J.; Raithby, P. R.; Younus, M.; White, A. J. P.; Williams, D. J.; Payne, N. N.; Yellowlees, L.; Beljonne, D.; Chawdhury, N.; Friend, R. H. *Organometallics* **1998**, *17*, 3034−3043 and references therein.

(36) Zhu, Y.; Clot, O.; Wolf, M. O.; Yap, G. P. A. *J. Am. Chem. Soc.* **1998**, *120*, 1812−1821.

(37) Nelsen, S. F.; Tran, H. Q.; Nagy, M. A. *J. Am. Chem. Soc.* **1998**, *120*, 298−304.

(38) Lambert, C.; Nöll, G. *J. Am. Chem. Soc.* **1999**, *121*, 8434−8442.

(39) Creutz, C.; Newton, M. D.; Sutin, N. *J. Photochem. Photobiol. A: Chem.* **1994**, *82*, 47−59.

(40) Curtis, J. C.; Sullivan, B. P.; Meyer, T. J. *Inorg. Chem.* **1983**, *22*, 224−236.

Table 3. LMCT Band Parameters in Oxidized Complexes

complex	$\nu_{max} \pm 50$ (cm^{-1})	ϵ_{max} ($M^{-1}\,cm^{-1}$)	$\Delta\nu_{1/2} \pm 100$ (cm^{-1})	$f \times 10^3$ (cm^{-1})[a]
1a$^+$	11430	630 ± 20	3460	10 ± 2
1b$^+$	9850	1390 ± 50	3680	24 ± 2
1c$^+$	9130	1550 ± 70	3800	27 ± 2
1d$^+$	10040	1190 ± 50	3240	18 ± 2
1e$^+$	7782	2090 ± 90	3750	36 ± 2
2a^{2+}	11300	1550 ± 60	3805	27 ± 2
2b^{2+}	9900	2600 ± 100	3890	46 ± 2
2c^{2+}	9260	3600 ± 160	3760	62 ± 3
2d^{2+}	10150	2400 ± 90	4120	46 ± 2
2e^{2+}	7970	4000 ± 150	4300	79 ± 3

[a] From eq 2.

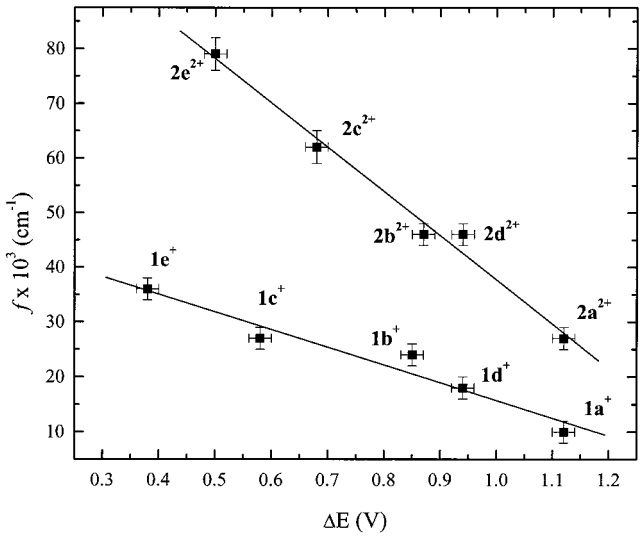

Figure 4. Oscillator strength of the near-IR transition (f) vs oxidation potential difference (ΔE) for **1a**$^+$−**e**$^+$ and **2a**$^{2+}$−**e**$^{2+}$.

ing a Gaussian peak shape, we can calculate the oscillator strength, f, of the band from eq 2 where $\Delta\nu_{1/2}$ is the bandwidth at half-height.[20] The LMCT band parameters are collected in Table 3. A plot of f as a function of ΔE (Figure 4) shows a linear correlation both within the series of monoferrocenyl cations as well as within the diferrocenyl cations. The oscillator strengths of the dications are approximately twice those of the monocations due to the presence of twice the number of chromophores per molecule in the dications. From these plots it is clear that a smaller difference in oxidation potentials between donor and acceptor gives a greater charge-transfer transition oscillator strength.

$$f = (4.6 \times 10^{-9})\epsilon_{max}\Delta\upsilon_{1/2} \qquad (2)$$

The significance of the correlations observed between ν_{max} and f vs ΔE lies in the relationship between the intensity and shape of a charge-transfer band and the extent of charge delocalization. The delocalization coefficient or interaction parameter α^2 is proportional to the amount of time spent by an electron in a given site.[20,43] For a one-electron system, the oscillator strength and absorption band maximum are related to the charge-transfer dipole moment M by eq 3.[21] Here G is the degeneracy of the states concerned and e is the electric charge.

$$M^2 = \frac{e^2 f}{(1.085 \times 10^{11})G\upsilon_{max}} \qquad (3)$$

From eq 3 and the correlations in Figure 4 and between ν_{max} and ΔE it is clear that in the series of compounds studied here M^2 also correlates with ΔE. A smaller difference in donor and acceptor oxidation potentials results in a larger charge-transfer dipole moment. The dipole moment is related to the extent of delocalization α^2 and the transition dipole length R in cm by eq 4.[21]

$$M^2 \cong a^2 e^2 R^2 \qquad (4)$$

For complexes in which R is approximately the same, a larger dipole moment will therefore correlate to a larger α^2. Although we do not know the value of R here, it is reasonable that R will not vary significantly within the four pairs of complexes in the series with the same length oligothiophene group but with different substitution (for example **1a**$^+$ and **1d**$^+$, or **2c**$^{2+}$ and **2e**$^{2+}$). In these pairs, a direct correlation between the extent of charge delocalization and the dipole moment, and therefore ΔE, can be made. In each pair, the complex with the smaller ΔE has a larger oscillator strength and lower absorption maximum for the LMCT transition. Therefore, in each pair, a decrease in the oxidation potential gap between donor and acceptor results in greater charge delocalization.

We can also use eqs 3 and 4 to consider the effect of extending the length of the oligothiophene ligand on charge delocalization. As the length is increased (e.g. **1a**$^+$−**1c**$^+$) the oscillator strength increases and the absorption energy decreases, together giving a larger dipole moment. Here, it is reasonable that R would not be the same for all the complexes so we can conclude only that the *product* of the charge delocalization and R increases with an increase in the length of the oligothiophene ligand. Thus, either charge is more delocalized (if R does not change significantly) or charge is delocalized further along the rigid oligothiophene ligand (if α^2 does not change significantly). Either situation is desirable in a polymer because choosing a longer oligothiophene bridge which has an oxidation potential closer to that of the metal group will result either in greater delocalization of charge or in charge being delocalized over a greater length along the conjugated backbone.

These results have important implications for the design of metal-containing conjugated polymers in which the metal is redox active. It is clearly desirable to match the oxidation potentials of bridge and metal as closely as possible. Swager has also demonstrated that "redox-matching" in electropolymerized Co-salen systems and in polymetallorotaxanes results in higher conductivities.[8,15,16] The results of our study suggest that this concept is more general for materials in this class. This work also makes important links between electron-transfer in charge-transfer complexes and conducting polymers and oligomers, and contributes to understanding the relationships between these related processes.[34]

Acknowledgment. We thank the Natural Sciences and Engineering Research Council of Canada for support of this research.

Supporting Information Available: Full experimental details of the synthesis and characterization of **1a**−**e** and **2a**−**e**, cyclic voltammograms of **2a**−**2e**, vis−near-IR spectra of **2a**$^{2+}$−**e**$^{2+}$, and plots of absorption maxima vs oxidation potential difference for **1a**$^+$−**e**$^+$ and **2a**$^{2+}$−**e**$^{2+}$ (PDF). This material is available free of charge via the Internet at http://pubs.acs.org.

JA0008564

(41) Dodsworth, E. S.; Lever, A. B. P. *Chem. Phys. Lett.* **1984**, *112*, 567−570.
(42) Crutchley, R. J.; McCaw, K.; Lee, F.; Gabe, E. J. *Inorg. Chem.* **1990**, *29*, 2576−2581.
(43) Robin, M. B.; Day, P. *Adv. Inorg. Chem. Radiochem.* **1967**, *10*, 247−422.